Electronic Supplementary Material (ESI) for ChemComm.
This journal is © The Royal Society of Chemistry 2018

ELECTRONIC SUPPORTING INFORMATION

Phosphorescent Pt(II) complexes spatially arrayed in micellar polymeric nanoparticles providing dual readout for multimodal imaging

Maria T. Proetto,* Jan Sanning, Martin Peterlechner, Martin Thunemann, Linda Stegemann, Sanaz Sadegh, Anna Devor, Nathan C. Gianneschi* and Cristian A. Strassert*

Contents

1. General materials and methods

All reagents were purchased from VWR, Alfa Aesar or Sigma-Aldrich and used without further purification. Column chromatography was performed with silica gel 60 (particle size 35-70 μm, 230-400 mesh, Merck). NMR and mass spectra were measured by the Department of Organic Chemistry, University of Münster and at the Department of Chemistry and Biochemistry, University California San Diego. NMR spectra were recorded on an DPX/Avance 300 MHz, an Avance 400 from Burker Analytische Messtechnik (Karlsruhe, Germany) for some of the Pt(II) complexes, the ligands and their precursors and on an DD2 600 MHz from Agilent for Pt(II) complexes or a Varian Mercury Plus spectrometer 400 MHz. The ^{1}H NMR chemical shifts (δ) of the signals are given in parts per million and referenced to residual protons in the deuterated solvents: DMSO-d_6 (2.50 ppm), CD_2Cl_2-d_2 (5.32 ppm), $CDCl_3$-d (7.26 ppm), THF-d_8 (3.58 ppm), DMF-d_7 (8.03 ppm), CD_3COCD_3-d_6 (2.04 ppm). The ^{19}F NMR chemical shifts are referenced to $CFCl_3$ as an internal standard. The signal multiplicities are abbreviated as follows: s, singlet; d, doublet; t, triplet; q, quartet; m, multiplet. All coupling constants (*J*) are given in Hertz. High resolution mass spectrometry (HRMS) was performed via electrospray ionization (ESI) on a Bruker Daltonics MicroTof with loop injection. Sealed ampules of DMF-d_7 (Cambridge Isotopes) were used without further purification. Modified second generation Grubbs' ruthenium initiator, $(IMesH_2)(C_5H_5N)_2(Cl)_2Ru{=}CHPh$, was prepared as previously described (Sanford *et al. Organometallics*, **2001**, *20*, 5314). Polymerizations were performed under a dry N_2 atmosphere. Polymer dispersities and molecular weights were determined by size-exclusion chromatography (Phenomenex Phenogel 5u 10, 1k-75k, 300 x 7.80 mm in series with a Phenomex Phenogel 5u 10, 10K-1000K, 300 x 7.80 mm (0.05 M LiBr in DMF)) using a Shimadzu pump equipped with a multi-angle light scattering detector (DAWN-HELIOS: Wyatt Technology) and a refractive index detector Wyatt Optilab TrEX normalized to a 30,000 MW polystyrene standard. Particle diameters were determined by dynamic light scattering (DLS, D_{DLS}) using a Wyatt Dynapro NanoStar. Dry state TEM images of the nanoparticles were acquired on carbon grids (Ted Pella, INC.) on a FEI Tecnai G2 Sphera at 200 KV. Cell sectioning was performed by the UCSD School of Medicine Cellular & Molecular Medicine Electron Microscopy Core Facility. Cell TEM images were acquired on carbon grids (Ted Pella, Inc.) and obtained on a JEOL 1200 EX II TEM at 80 kV. TEM-EDX (Energy Dispersive X-Ray) was accomplished using a Zeiss Libra 200FE (at 200 kV) equipped with a corrected in-column Omega energy filter and a Noran EDX detector. Bright-field (BF), dark-field (DF) and diffraction pattern were recorded using a Gatan US4000 CCD and an energy slit of approximately 30 eV symmetrically around the zero loss. High-angle annular dark-field (HAADF) images were recorded using a Fischione Model3000 and a detection angle range of about 70 to 300 mrad. Energy-filtered TEM was applied using the tree-window method at the Pt-O and Pt-N edges with an exponential background model and window sizes of typical 8 eV. For the cell TEM experiments, cell sectioning was performed by the UCSD School of Medicine Cellular & Molecular

Medicine Electron Microscopy Core Facility. Cell TEM images were acquired on carbon grids (Ted Pella, Inc.) and obtained on a JEOL 1200 EX II TEM at 80 kV. For two-photon laser scanning microscopy (TPLSM), a two-photon laser scanning microscope (Ultima, Bruker Fluorescence Microscopy) equipped with a Ti:Sapphire laser (Ultra II, Coherent) tuned to 750 nm, and an Olympus 20x water immersion objective (XLUMPlanFLNXW, NA=1.0) were used. Signals were collected with a cooled GaAsP photomultiplier (H7422P-40, Hamamatsu) after passing through a 490-560 nm bandpass filter. Images were acquired with a dwell time of 2.8-4.4 µs at 512x512 pixels per image and variable (4-16x) zoom settings.

2. Synthesis

Synthetic procedures

Synthesis of *N*-(2-aminoethyldiisopropylamine)-5-norbornene-*exo*-2,3-dicarboxylic acid imide (**M_{am}**)

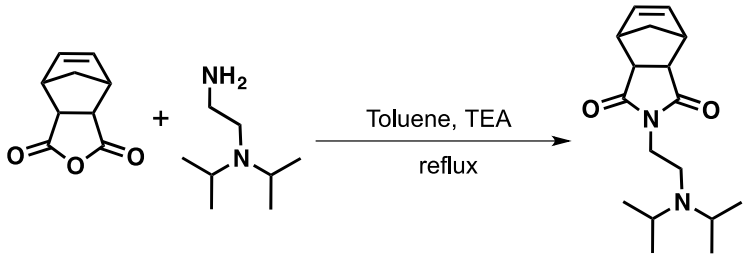

To a stirred solution of 2-aminoethyldiisopropylamine (648 mg, 4.5 mmol) in dry toluene (50 mL) was added 5-norbornene-*exo*-2,3-dicarboxylic anhydride (492 mg, 3 mmol) and triethylamine (606 mg, 6 mmol). The reaction was heated to reflux overnight. The solvent was reduced to a minimum under reduced pressure and was in a vacuum pump for further 5 h to yield a brown oil (860 mg, 99%). ^{1}H NMR (400 MHz, Cl_3CD-*d*) δ 6.27 (m, 2H), 3.47 (t, 2H), 3.26 (m, 2H), 3.01 (m, 2H), 2.66 (m, 2H), 2.57 (t, 2H), 1.50 (d, 1H), 1.34 (d, 1H), 0.97 (d, 12H). HRMS (ESI+, MeOH, *m/z*) calcd. for $[M + H]^+$ 291.2067, found 291.2063 ($[M + H]^+$).

General procedure for the synthesis of *N*-(pyridin-4-ylmethyl)hexanamide)-5-norbornene-*exo*-2,3-dicarboxylic acid imide (**L_{anc}**)

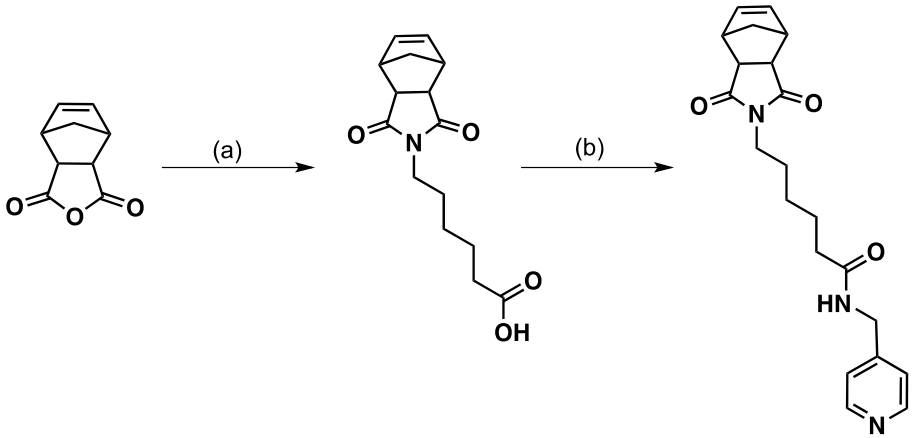

***Scheme S1**. Synthetic route towards the L_{anc} ligand. (a) 6-Aminohexanoic acid, triethylamine, toluene, reflux, 24 h. (b) 4-(Aminomethyl)pyridine, CDMT, NMM, DMF, 0 °C to rt, 24 h.*

Synthesis of *N*-(6-hexanoic acid)-5-norbornene-*exo*-2,3-dicarboxylic acid imide

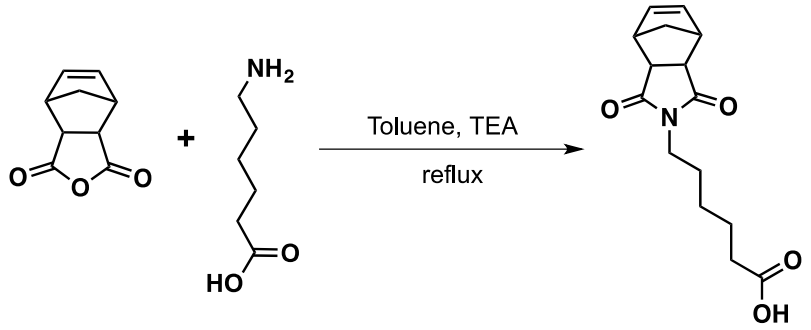

To a stirred solution of 6-aminohexanoic acid (1.73 g, 13.2 mmol) in dry toluene (100 mL) was added 5-norbornene-*exo*-2,3-dicarboxylic anhydride (1.97 g, 12 mmol) and triethylamine (1.33 g, 13.2 mmol). The reaction, equipped with a Dean-Stark trap, was heated to reflux overnight. After cooling to rt, the solvent was reduced to a minimum under reduced pressure. The mixture was resuspended in dichloromethane and successively washed twice with 1 M HCl and twice with brine. The organic layer was dried over $CaSO_4$ and the solvent evaporated to afford a white solid (3.46 g, 99%). ^{1}H NMR (400 MHz, CD_3COCD_3-d_6) δ 6.32 (m, 2H), 3.41 (t, 2H), 3.14 (m, 2H), 2.68 (m, 2H), 2.28 (t, 2H), 1.64-1.22 (m, 8H). HRMS (ESI+, MeOH, *m/z*) calcd. for $[M + Na]^+$ 300.1206, found 300.1207 ($[M + Na]^+$).

Synthesis of *N*-(pyridin-4-ylmethyl)hexanamide)-5-norbornene-*exo*-2,3-dicarboxylic acid imide (**L$_{anc}$**)

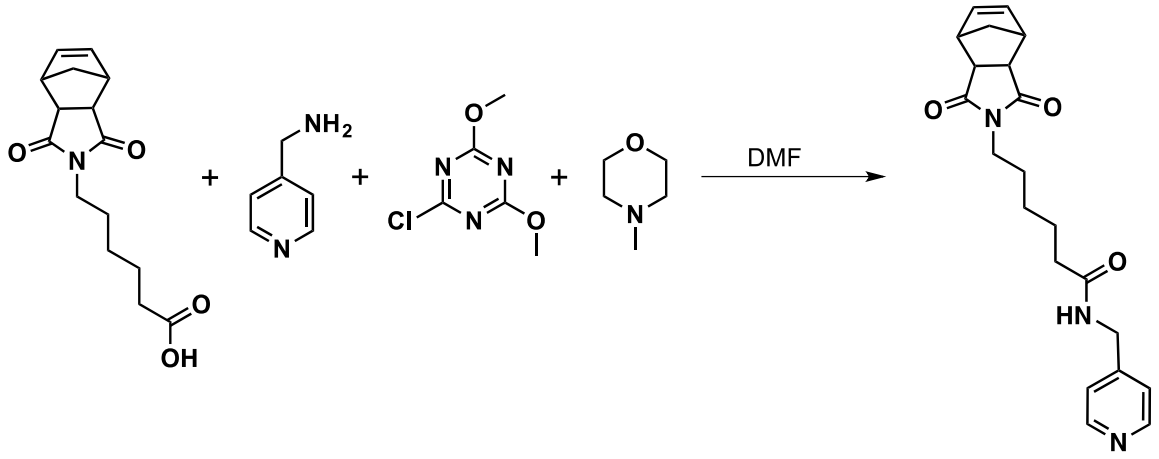

In a 50 mL flask *N*-(6-hexanoic acid)-5-norbornene-*exo*-2,3-dicarboxylic acid imide (1.11 g, 4 mmol) was dissolved in 25 mL DMF. 2,4,6-chlorodimethoxytriazine (CDMT, 714 mg, 4.08 mmol) was added. The reaction mixture was cooled to 0 °C with an ice bath and N-methylmorpholine (439 µl, 4 mmol) was added. The mixture reacted at 0 °C for 5 h and then 4-(aminomethyl)pyridine (427 mg, 2.02 mmol) and N-methylmorpholine (439 µl, 4 mmol) dissolved in 10 mL DMF were added.

The mixture reacted under stirring for 2 h at 0 °C and then for overnight at r.t. The solvent was evaporated under reduced pressure and the residue was dissolved in ethyl acetate. The solution was successively washed with water, saturated $NaHCO_3$ solution, saturated NaCl solution and water. The organic layer was dried over $CaSO_4$ and the solvent evaporated. The final product was isolated by column chromatography (75% hexanes, 25% ethyl acetate) to yield a yellow solid (171 mg, 11%). ^{1}H NMR (400 MHz, CD_3COCD_3-d_6) δ 8.56 (m, 2H), 7.19 (m, 2H), 6.29 (m, 2H), 5.96 (s, 1H), 4.46 (m, 2H), 3.46 (t, 2H), 3.26 (m, 2H), 2.66 (m, 2H), 2.26 (t, 2H), 1.72-1.19 (m, 8H). HRMS (ESI+, MeOH, *m/z*) calcd. for [$[M + Na]^+$ 368.1969, found, 368.1966 ($[M + Na]^+$).

General Procedure for the Synthesis of the polymerizable Pt(II) Complex (**M_{Pt}**)

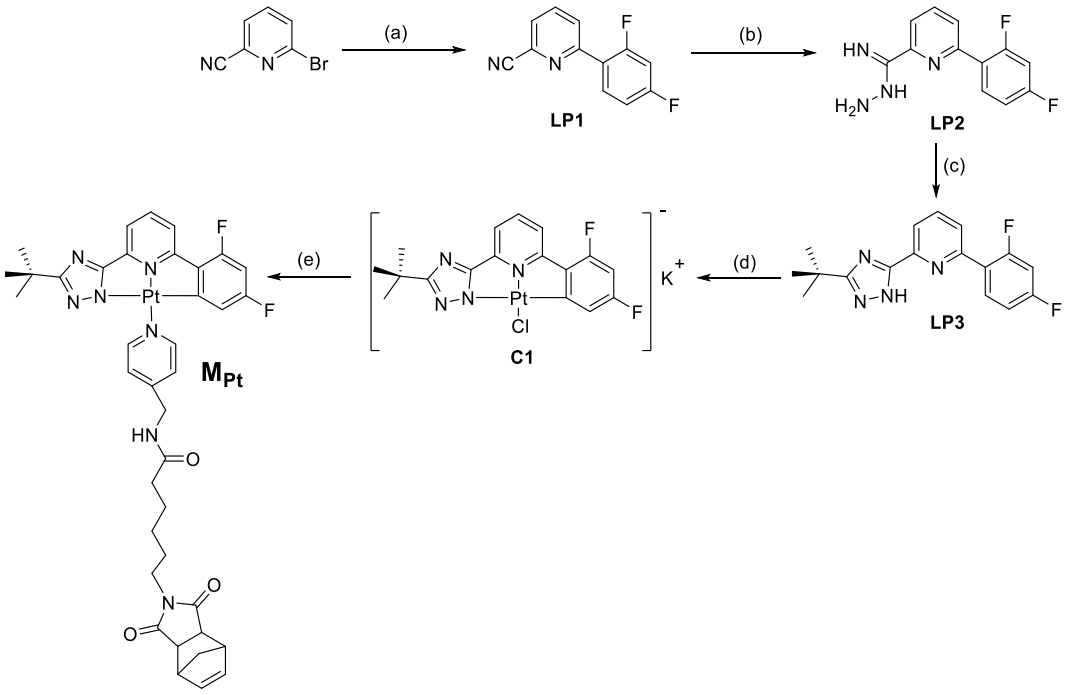

***Scheme S2**. Synthetic route towards the C^N^N ligand precursor **LP3** and the corresponding Pt(II) complex **M_{Pt}**. (a) 2,4-Difluorophenylboronic acid, $Pd(PPh_3)_4$, K_2CO_3, THF, N_2, reflux, 24 h. (b) N_2H_4 x H_2O, EtOH, rt. (c) 1) (tBu)C(O)Cl, K_2CO_3, DMF, 0°C to rt, 2) ethylene glycol, 160°C. (d) K_2PtCl_4, acetic acid, reflux. (e) **L_{anc}**, THF.*

The ligand precursors **LP1**, **LP2** and **LP3** as well as complex **C1** were synthesized as previously described by Sanning *et al*. (*J. Mater. Chem. C.* **2016**, *4*, 2560). Complex **C1** (0.172 mmol) was suspended in THF (15 mL). Next, the reaction mixture was degassed intensely, before L_{anc} (0.172 mmol) was added. After the reaction was stirred at 50 °C for 12 h in a nitrogen atmosphere it was cooled down and absorbed onto silica gel by removing the solvent under reduced pressure. This was loaded onto a column packed with silica gel, and a column chromatographic separation was performed using THF / acetone / (cyclo)hexane as the eluent to give the final product as an

orange solid, 13%. ^{1}H NMR (300 MHz, CD_2Cl_2-d_2) δ 8.75 (d, *J* = 6.5 Hz, 2H), 7.76 (t, *J* = 8.0 Hz, 1H), 7.56 (dd, *J* = 15.1, 8.1 Hz, 2H), 7.42 (d, *J* = 5.9 Hz, 2H), 6.50 (ddd, *J* = 11.7, 9.1, 2.2 Hz, 1H), 6.26 (s, 2H), 5.79 (dd, *J* = 8.4, 2.2 Hz, 1H), 4.65 (d, *J* = 16.7 Hz, 1H), 4.28 (d, *J* = 16.7 Hz, 1H), 2.98 – 2.84 (m, 2H), 2.73 – 2.51 (m, 2H), 2.33 (d, *J* = 8.7 Hz, 1H), 1.47 (d, *J* = 8.5 Hz, 1H), 1.37 (s, 9H). ^{19}F NMR (282 MHz, CD_2Cl_2-d_2) δ -104.08, -108.56. HRMS (ESI+, MeOH, *m/z*) calcd. for $[M + H]^+$ 762.19647, found, 762.19656 ($[M + H]^+$); calcd. for $[M + H_2O + H]^+$ 780.20704, found, 780.20709 ($[M + H_2O + H]^+$); calcd. for $[M + H_2O + Na]^+$ 802.18929, found, 802.18910 ($[M + H_2O + Na]^+$).

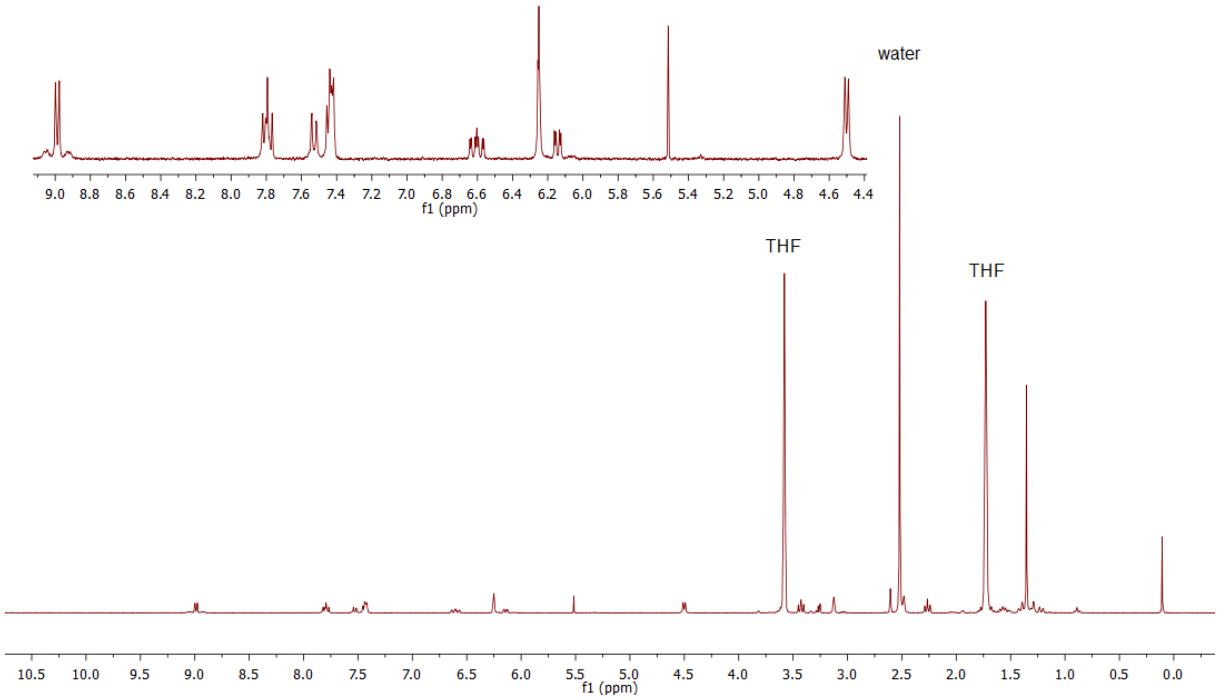

Figure S1. *^{1}H-NMR spectrum of* ***M_{Pt}****.*

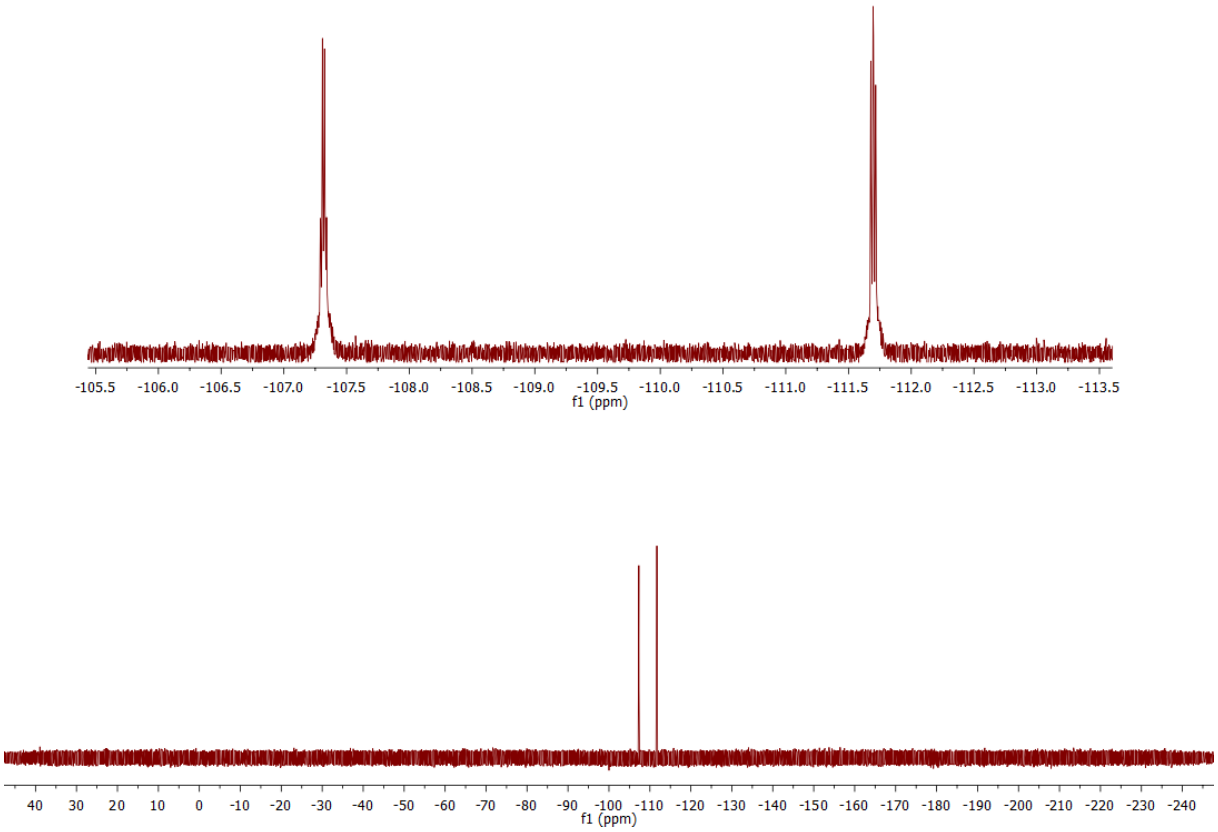

Figure S2. *^{19}F-NMR spectrum of* ***M$_{Pt}$****.*

Synthesis of the polymer **P$_{shell}$**

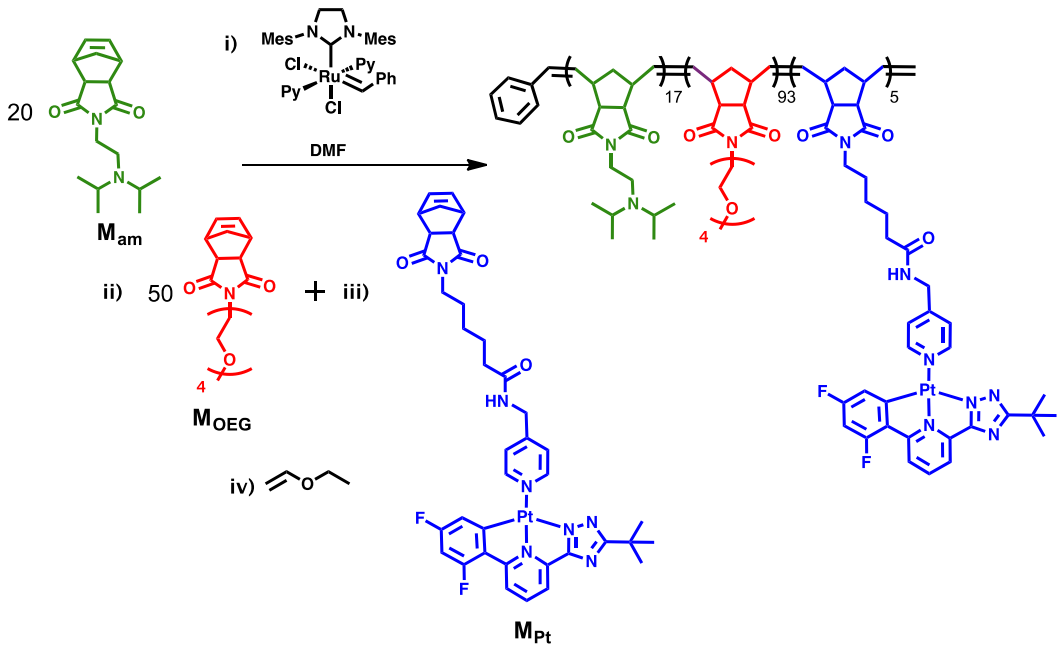

To a stirred solution of $\mathbf{M_{am}}$ (6.4 mg, 0.0220 mmol) in dry DMF (550 µL) was added a solution of modified second generation Grubbs' ruthenium catalyst (0.8 mg, 0.001 mmol) in dry DMF (110 µL). The reaction was left to stir under a N_2 atmosphere for 30 min. 60 µL were removed and quenched with ethyl vinyl for SEC-MALS analysis. A solution of the hydrophilic OEG-monomer, $\mathbf{M_{OEG}}$ (17.6 mg, 0.05 mmol) in DMF (100 µL) was added to the remaining reaction mixture and stirred for additional 30 min. 50 µL were removed and quenched with ethyl vinyl for SEC-MALS analysis. A solution of $\mathbf{M_{Pt}}$ (0.8 mg, 0.001 mmol) in DMF (100 µL) was added to the remaining reaction mixture. The mixture was left to stir under a N_2 atmosphere for additional 30 min, followed by ethyl vinyl ether quenching (5 µL). After 25 min the polymer was crashed out over cold ether to give a brown solid.

Synthesis of the polymer $\mathbf{P_{core}}$

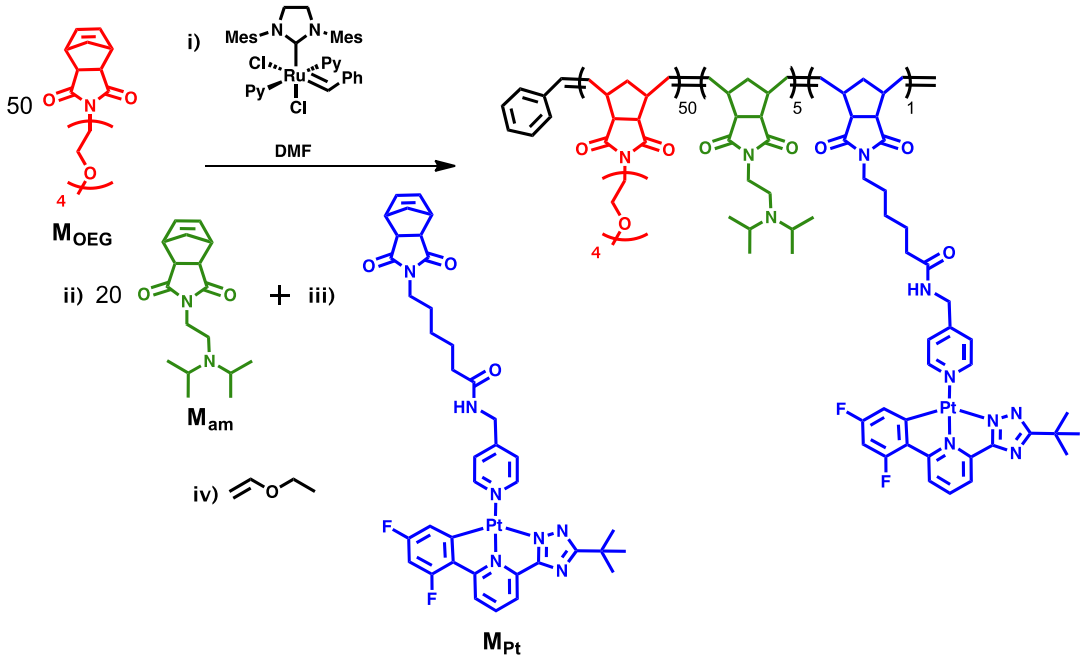

To a stirred solution of $\mathbf{M_{OEG}}$ (19.5 mg, 0.055 mmol) in dry DMF (550 µL) was added a solution of modified second generation Grubbs' ruthenium catalyst (0.8 mg, 0.001 mmol) in dry DMF (110 µL). The reaction was left to stir under a N_2 atmosphere for 30 min. 60 µL were removed and quenched with ethyl vinyl for SEC-MALS analysis. A solution of the hydrophobic monomer, $\mathbf{M_{am}}$ (5.8 mg, 0.02 mmol) in DMF (100 µL) was added to the remaining reaction mixture and stirred for additional 30 min. 50 µL were removed and quenched with ethyl vinyl for SEC-MALS analysis. A solution of $\mathbf{M_{Pt}}$ (0.8 mg, 0.001 mmol) in DMF (100 µL) was added to the remaining reaction mixture. The mixture was left to stir under a N_2 atmosphere for additional 30 min, followed by ethyl vinyl ether quenching (5 µL). After 25 min the polymer was crashed out over cold ether to give a brown solid.

Spherical NP formation

Each polymer (1 mg) was dissolved in DMF (1000 µL). 1000 µL of a 50:50 mixture of DMF:PBS 0.1X was added slowly over the course of 5 h. This suspension was dialyzed against 0.1X PBS through a 3.5 kDa MWCO for 2 days. The 0.1X PBS was changed twice over that time.

Time-dependent polymerization of $\mathbf{M_{Pt}}$

4.4 mg of $\mathbf{M_{Pt}}$ (0.005 mmol) and 2.5 mg of N-benzyl-5-norborene-*exo*-2,3-dicarboximide (0.01 mmol) were dissolved in 500 µL DMF-d_7 in a NMR tube. A solution of the modified second generation Grubbs' ruthenium catalyst (0.3 mg, 0.005 mmol) in dry DMF (100 µL) was added and the polymerization was controlled over time by NMR.

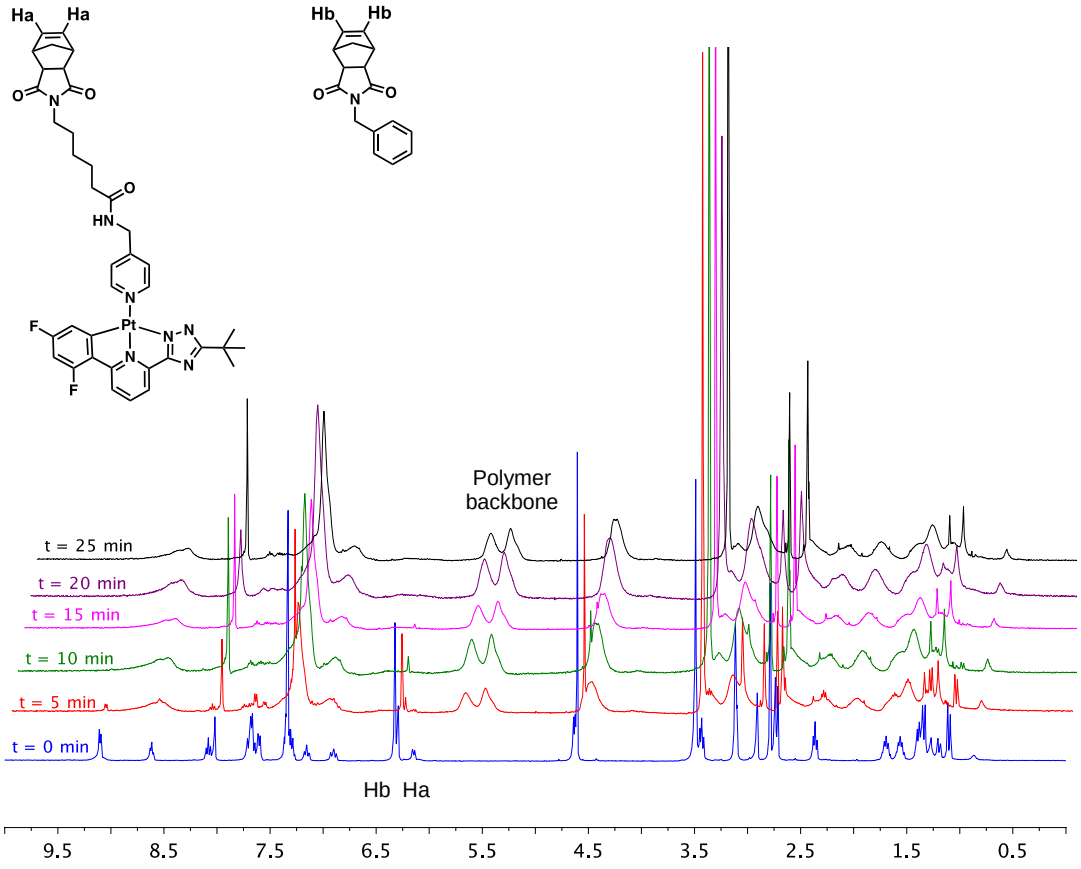

Figure S3. *Time-dependent ^{1}H NMR (chemical shifts expressed in ppm). In order to provide efficient polymerization by avoiding steric problems, the* $\boldsymbol{M_{Pt}}$ *was copolymerized with a phenyl monomer as a breed 1:2 mixture the phenyl monomer. The olefin peaks of* $\boldsymbol{M_{Pt}}$ *(Ha, 6.15 ppm) and the ones of the phenyl-monomer (Hb, 6.31 ppm) disappear within 20 min, confirming complete polymerization.*

3. Size Exclusion Chromatography – Multi-Angle Light Scattering (SEC-MALS) analysis

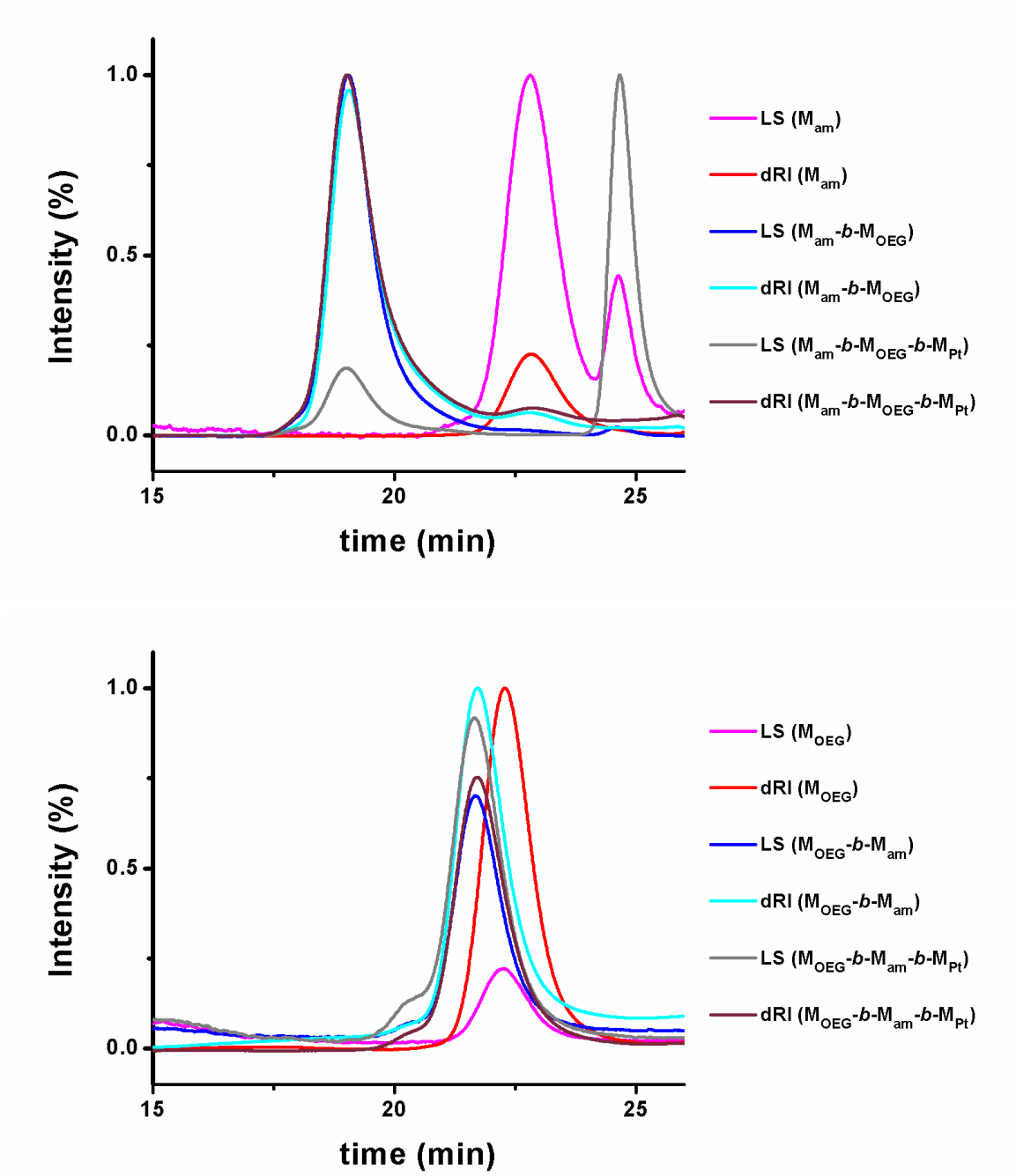

Figure S4. *SEC-MALS plots expressed as relative intensity vs. time for the polymers obtained as the polymerization of monomers* $\boldsymbol{M_{am}}$ *and* $\boldsymbol{M_{OEG}}$ *and the subsequent polymerization of monomer* $\boldsymbol{M_{Pt}}$ *to give polymers* $\boldsymbol{P_{shell}}$ *(top) and* $\boldsymbol{P_{core}}$ *(bottom).*

Table S1. Physical characteristics of polymers $\mathbf{P_{shell}}$ and $\mathbf{P_{core}}$ determined by SEC-MALS

	Polymer identity	M_n [g mol^{-1}]	M_w [g mol^{-1}]	$Đ_M$
	$\mathbf{Mam}_{17}$	5.01 x10^3	5.03 x10^3	1.003
	$\mathbf{Mam}_{17}$-*b*-$\mathbf{MOEG}_{93}$	3.70 x10^4	3.79 x10^4	1.024
$\mathbf{P_{shell}}$	$\mathbf{Mam}_{17}$-*b*-$\mathbf{MOEG}_{93}$-*b*-$\mathbf{MPt}_5$	4.19 x10^4	4.20 x10^4	1.006
	$\mathbf{MOEG}_{50}$	1.64 x10^4	1.79 x10^4	1.095
	$\mathbf{MOEG}_{50}$-*b*-$\mathbf{Mam}_5$	1.89 x10^4	1.90 x10^4	1.006
$\mathbf{P_{core}}$	$\mathbf{MOEG}_{50}$-*b*-$\mathbf{Mam}_5$-*b*-$\mathbf{MPt}_1$	1.98 x10^4	1.99 x10^4	1.009

4. Size analysis by Dynamic Light Scattering (DLS) and TEM

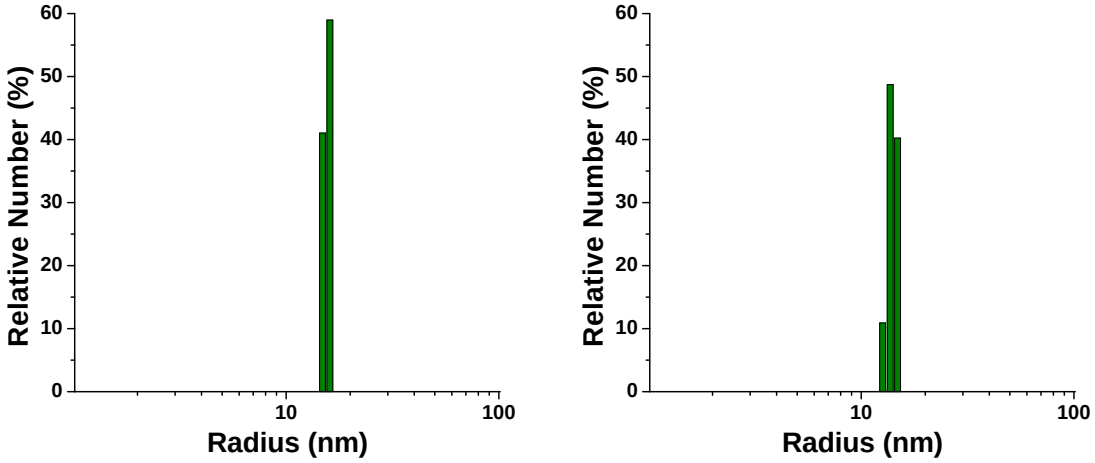

Figure S5. *DLS size distribution plots of* ***NP$_{shell}$*** *(left, 31 nm diameter) and* ***NP$_{core}$*** *(right, 28 nm diameter) obtained for the dialysis of the polymers* ***P$_{shell}$*** *and* ***P$_{core}$*** *from DMF into water and expressed as percent intensity vs. hydrodynamic radius (nm).*

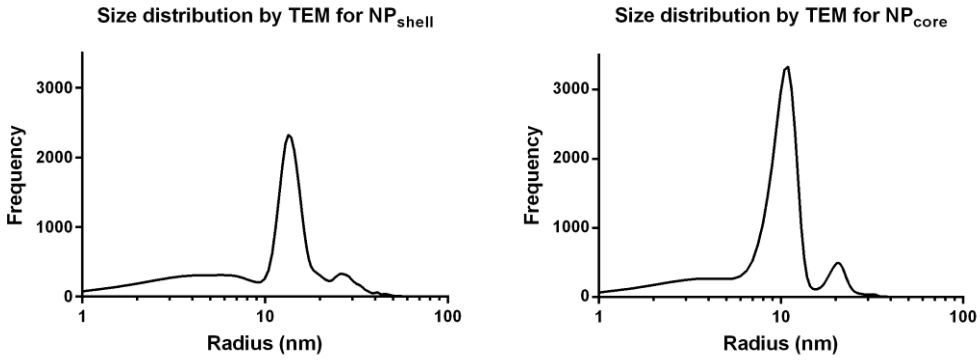

Figure S6. *TEM size distribution plots of* ***NP$_{shell}$*** *(left, 29 ± 6 nm diameter) and* ***NP$_{core}$*** *(right, 24 ± 9 nm diameter) obtained for the dialysis of the polymers* ***P$_{shell}$*** *and* ***P$_{core}$*** *from DMF into water and expressed as Frequency vs. radius (nm).*

5. Transmission Electron Microscopy (TEM) imaging of nanoparticles

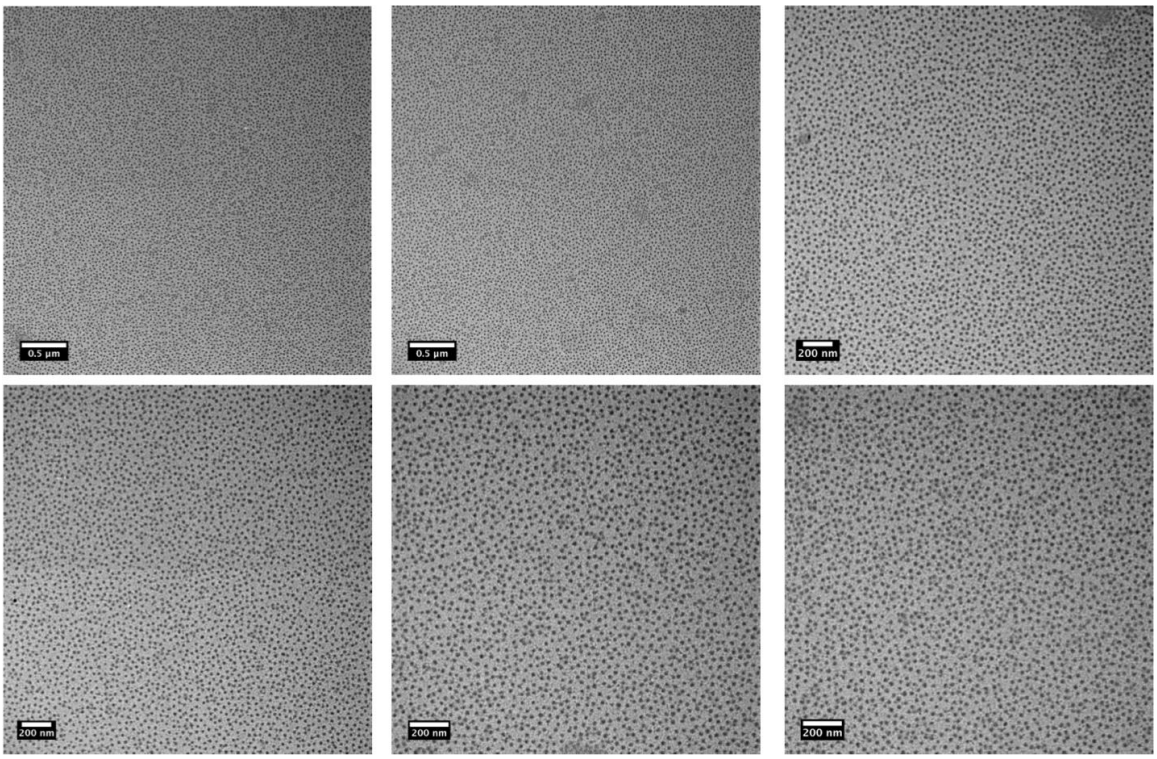

Figure S7. *Dry-state non-stained TEM images of* ***NP_{shell}.***

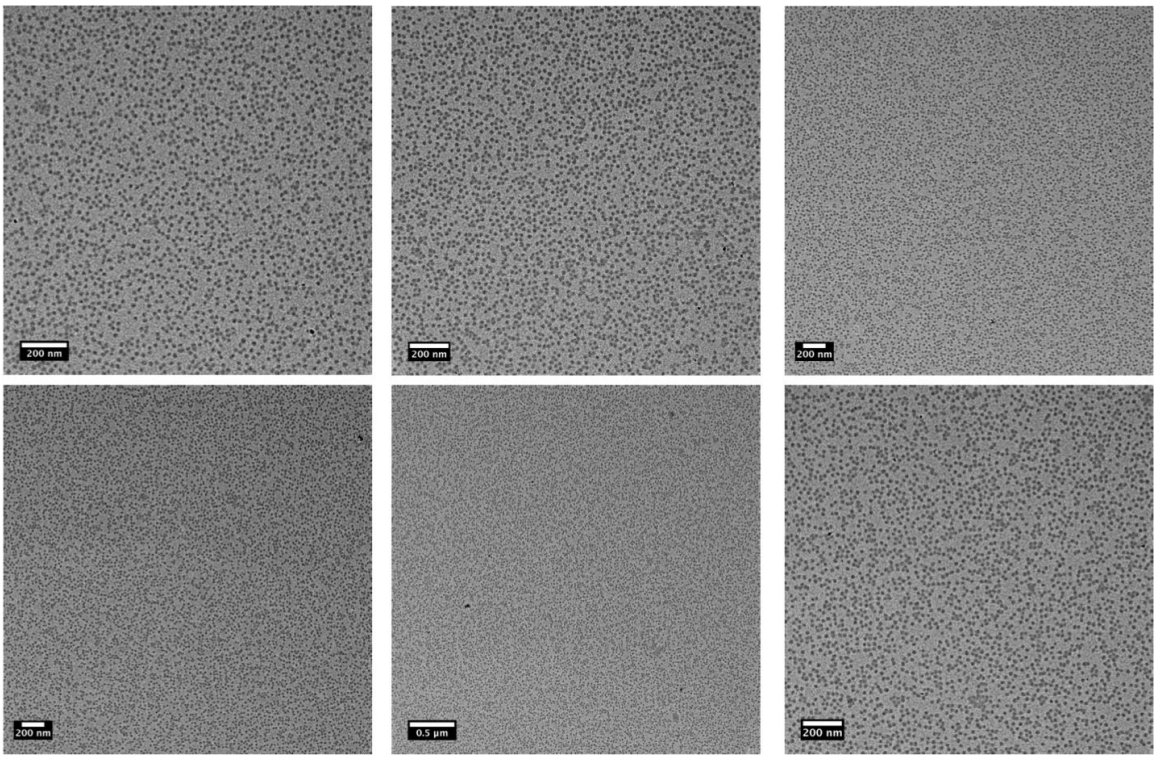

Figure S8. *Dry state non-stained TEM images of* ***NP_{core}.***

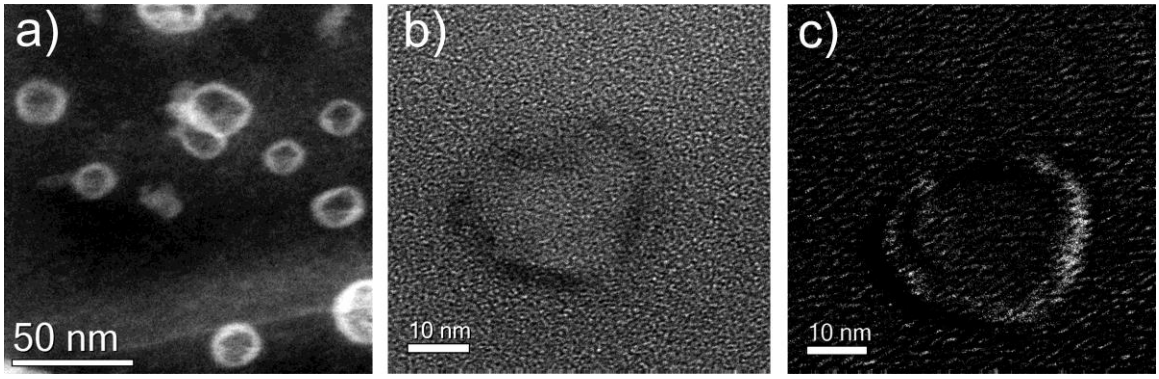

Figure S9. *TEM of* ***NP$_{shell}$****. The HAADF in a) shows high Z-contrast in the shell of the particles. A selected particle was analyzed using BF-imaging b). A weak diffraction contrast is visible. EFTEM analysis of the particle in b) using the three-window-method of the Pt-O-edge shows an enrichment of Pt at the shell in c).*

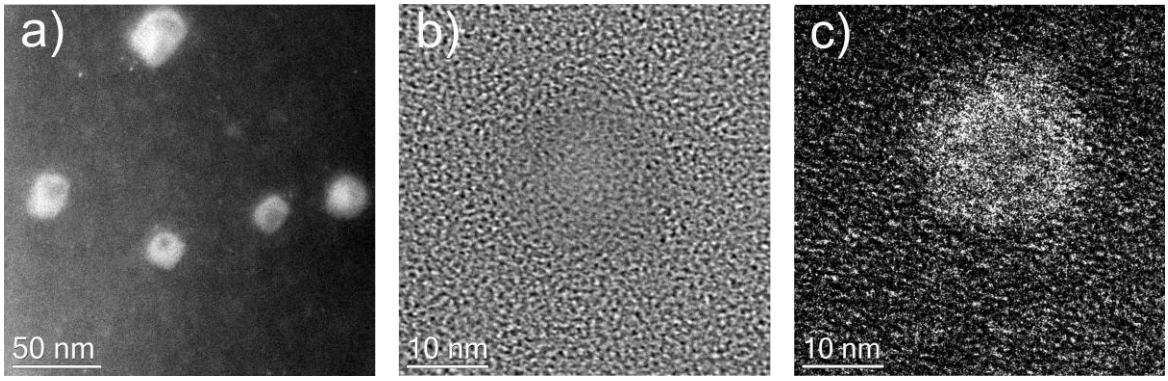

Figure S10. *TEM of* ***NP$_{core}$****. The HAADF in a) shows bright Z-contrast across the particles. Minor deviations of the Z-contrast might be attributed to Pt-aggregation. One selected particle was analyzed using BF-imaging b). A weak diffraction contrast of this comparably small particle on a carbon substrate is visible. EFTEM analysis of the particle in b) using the three-window-method of the Pt-O-edge shows a fairly homogenous distribution of Pt in c).*

As visible in the HAADF, the **NP$_{shell}$** show bright contrast in the shell. Since HAADF is based on scattering contrast, this shows that the shell gives a stronger scattering than the core, due to a higher Z-number of the atoms and/or a larger number of atoms. Diffraction contrast as obtained by BF-imaging is indicating a stronger ability for diffraction in the shell, as expected from an ordered structure. However, this contrast is not homogenous as it would appear if related to a single crystalline phase, and thus it is concluded that the ordering is below ~2 nm. The background-corrected EFTEM image acquired using an energy loss of a Pt-edge shows an enrichment of Pt in the shell, in agreement with the bright HAADF contrast of the shell arising from comparably heavy Pt atoms.

The HAADF of the **NP$_{core}$** shows, if compared to the **NP$_{shell}$**, a non-localized contrast across the particles. This originates from a rather homogenous distribution of strongly scattering atoms. The BF contrast is hardly detectable above the level of the amorphous carbon-substrate. Thus, it is concluded, that this diffracting structure is essentially disordered. Also for the **NP$_{core}$**, an EFTEM image using a Pt-edge was calculated taking the statistical background into account. The arising EFTEM contrast is essentially non-localized across the particle, indicating a homogenous distribution of Pt-across the particle.

The combination of the HAADF and the EFTEM information shows that not only the chemistry but also the density of these nanoparticles is basically homogenous on a length scale of nanometers. It should be noted that the **NP$_{core}$** and **NP$_{shell}$** particles have typically a size of 15-30 nm; however, there is within the statistical error a trend suggesting that the **NP$_{shell}$** particles are slightly larger.

6. Steady-state and time-resolved spectroscopy

Steady-state excitation and emission spectra were recorded on a FluoTime300 spectrometer from PicoQuant equipped with a 300 W ozone-free Xe lamp (250-900nm), a 10 W Xe flash-lamp (250-900 nm, pulse width < 10µs) with repetition rates of 0.1 – 300 Hz, an excitation monochromator (Czerny-Turner 2.7 nm/mm dispersion, 1200 grooves/mm, blazed at 300 nm), diode lasers (pulse width < 80 ps) operated by a computer-controlled laser driver PDL-820 (repetition rate up to 80 MHz, burst mode for slow and weak decays), two emission monochromators (Czerny-Turner, selectable gratings blazed at 500 nm with 2.7 nm/mm dispersion and 1200 grooves/mm, or blazed at 1250 nm with 5.4 nm/mm dispersion and 600 grooves/mm), Glan-Thompson polarizers for excitation (Xe-lamps) and emission, a Peltier-thermostatized sample holder from Quantum Northwest (-40°C – 105°C), and two detectors, namely a PMA Hybrid 40 (transit time spread FWHM < 120 ps, 300 – 720 nm) and a R5509-42 NIR-photomultiplier tube (transit time spread FWHM 1.5 ns, 300-1400 nm) with external cooling (-80°C) from Hamamatsu. Steady-state and fluorescence lifetimes were recorded in TCSPC mode by a PicoHarp 300 (minimum base resolution 4 ps). Emission and excitation spectra were corrected for source intensity (lamp and grating) by standard correction curves. Lifetime analysis was performed using the commercial FluoFit software. The quality of the fit was assessed by minimizing the reduced chi squared function ($\chi 2$) and visual inspection of the weighted residuals and their autocorrelation. Luminescence quantum yields were measured with a Hamamatsu Photonics absolute PL quantum yield measurement system (C9920-02) equipped with a L9799-01 CW Xenon light source (150 W), monochromator, C7473 photonic multi-channel analyzer, integrating sphere and employing U6039-05 PLQY measurement software (Hamamatsu Photonics, Ltd., Shizuoka, Japan). All solvents used were of spectrometric grade.

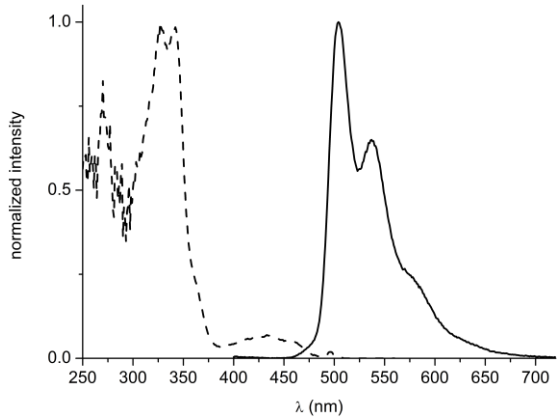

Figure S11. *Excitation (dashed line, emission at 495 nm) and emission (solid line, excitation at 250 nm) spectra of* $\mathbf{M_{Pt}}$ *(10^{-6} M) in fluid CH_2Cl_2 at room temperature.*

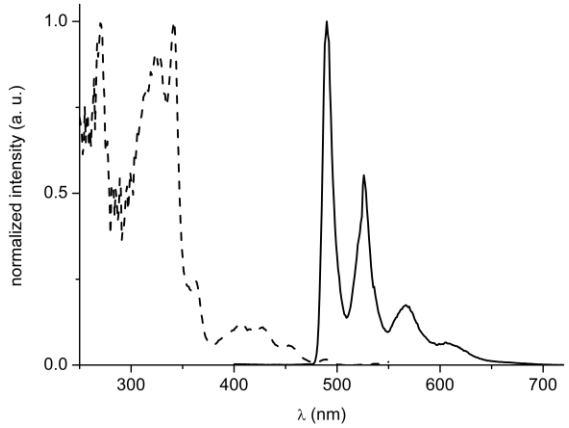

Figure S12. *Excitation (dashed line, emission at 580 nm) and emission (solid line, excitation at 340 nm) spectra of* $\mathbf{M_{Pt}}$ *(10^{-6} M) in a frozen glassy matrix of CH_2Cl_2:MeOH (1:1) at 77K.*

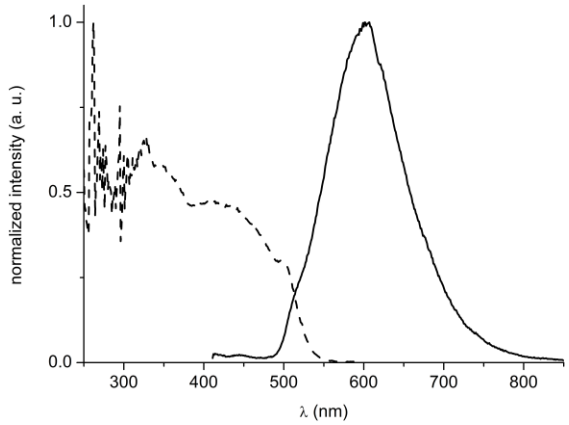

Figure S13. *Excitation (dashed line, emission at 580 nm) and emission (solid line, excitation at 340 nm) spectra of* $\mathbf{M_{Pt}}$ *in the solid state.*

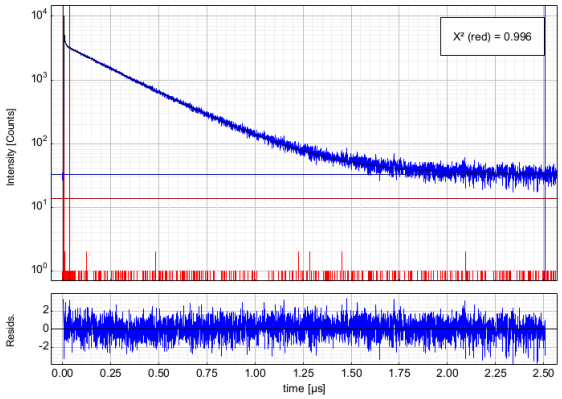

Parameter	Value	Conf. Lower	Conf. Upper
A_1 [Cnts]	4086.3	-33.1	+33.1
τ_1 [µs]	0.28372	-0.00180	+0.00180
A_2 [Cnts]	5714	-677	+677
τ_2 [µs]	0.002841	-0.000362	+0.000362
Bkgr. Dec [Cnts]	33.11	-1.35	+1.35
Bkgr. IRF [Cnts]	13.86	-1.16	+1.16
Shift IRF [µs]	0.0007827	-0.0000342	+0.0000342
A Scat [Cnts]	4460	-1470	+1470

Figure S14. *Left: Time-resolved photoluminescence decay of* ***M_{Pt}*** *(10^{-6} M) in aerated CH_2Cl_2 at room temperature including the residuals (λ_{exc} =376.7 nm, λ_{em}=505 nm). Right: Fitting parameters including pre-exponential factors and confidence limits.*

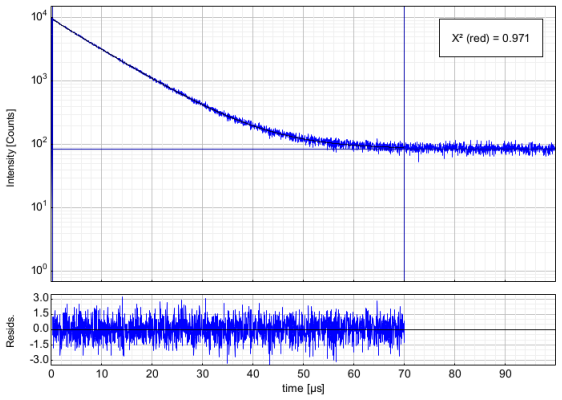

Parameter	Value	Conf. Lower	Conf. Upper
A_1 [Cnts]	9014.6	-42.2	+42.2
τ_1 [µs]	9.0765	-0.0334	+0.0334
A_2 [Cnts]	400.2	-98.6	+98.6
τ_2 [µs]	2.749	-0.813	+0.813
Bkgr. Dec [Cnts]	85.38	-2.29	+2.29

Figure S15. *Left: Time-resolved photoluminescence decay of* ***M_{Pt}*** *(10^{-6} M) in deaerated CH_2Cl_2 at room temperature including the residuals (λ_{exc} =376.7 nm, λ_{em}=505 nm). Right: Fitting parameters including pre-exponential factors and confidence limits.*

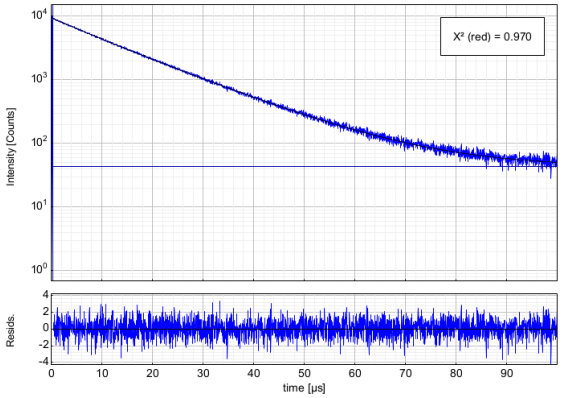

Parameter	Value	Conf. $_{Lower}$	Conf. $_{Upper}$
A_1 [Cnts]	7543.5	-38.1	+38.1
τ_1 [µs]	14.3644	-0.0538	+0.0538
A_2 [Cnts]	1538.6	-61.9	+61.9
τ_2 [µs]	7.968	-0.319	+0.319
Bkgr. $_{Dec}$ [Cnts]	43.10	-1.97	+1.97

Figure S16. *Left: Time-resolved photoluminescence decay of* $\mathbf{M_{Pt}}$ *(10^{-6} M) in a frozen glassy matrix of CH_2Cl_2:MeOH (1:1) at 77K including the residuals (λ_{exc} =376.7 nm, λ_{em}=505 nm). Right: Fitting parameters including pre-exponential factors and confidence limits.*

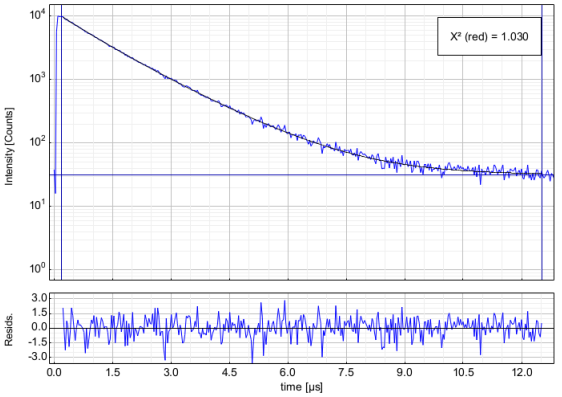

Parameter	Value	Conf. $_{Lower}$	Conf. $_{Upper}$
A_1 [Cnts]	5351.0	-40.6	+40.6
τ_1 [µs]	1.47957	-0.00784	+0.00784
A_2 [Cnts]	4172.9	-66.1	+66.1
τ_2 [µs]	0.8524	-0.0128	+0.0128
Bkgr. $_{Dec}$ [Cnts]	31.62	-1.48	+1.48

Figure S17. *Left: Time-resolved photoluminescence decay of* $\mathbf{M_{Pt}}$ *(10^{-6} M) in in the solid state including the residuals (λ_{exc} =376.7 nm, λ_{em}=505 nm). Right: Fitting parameters including pre-exponential factors and confidence limits.*

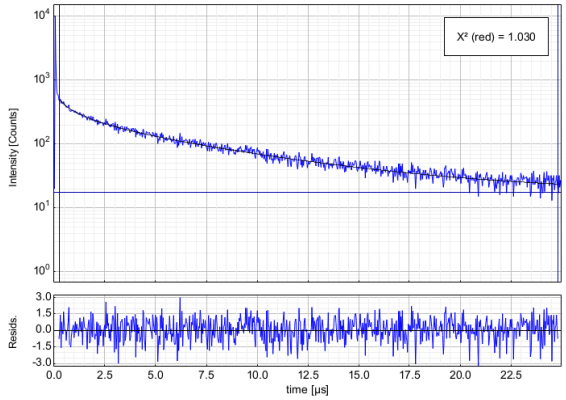

Parameter	Value	Conf. $_{Lower}$	Conf. $_{Upper}$
A_1 [Cnts]	214.94	-5.41	+5.41
τ_1 [µs]	6.902	-0.161	+0.161
A_2 [Cnts]	159.5	-16.5	+16.5
τ_2 [µs]	1.501	-0.177	+0.177
A_3 [Cnts]	109.9	-37.0	+37.0
τ_3 [µs]	0.374	-0.166	+0.166
Bkgr. $_{Dec}$ [Cnts]	17.52	-1.16	+1.16

Figure S18. *Left: Time-resolved photoluminescence decay of* ***NP$_{shell}$*** *including the residuals (λ_{exc} =376.7 nm, λ_{em}=500 nm). Right: Fitting parameters including pre-exponential factors and confidence limits.* ***NP$_{shell}$*** *were suspended in aerated 10% PBS at a concentration of 0.5 mg/mL.*

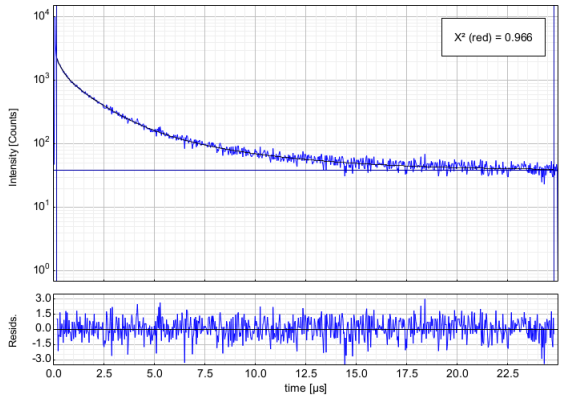

Parameter	Value	Conf. $_{Lower}$	Conf. $_{Upper}$
A_1 [Cnts]	221.05	-8.69	+8.69
τ_1 [µs]	4.964	-0.157	+0.157
A_2 [Cnts]	1083.4	-27.1	+27.1
τ_2 [µs]	1.4730	-0.0340	+0.0340
A_3 [Cnts]	841.1	-82.1	+82.1
τ_3 [µs]	0.2797	-0.0342	+0.0342
Bkgr. $_{Dec}$ [Cnts]	38.43	-1.27	+1.27

Figure S19. *Left: Time-resolved photoluminescence decay of* ***NP$_{shell}$*** *including the residuals (λ_{exc} =376.7 nm, λ_{em}=600 nm). Right: Fitting parameters including pre-exponential factors and confidence limits.* ***NP$_{shell}$*** *were suspended in deaerated 10% PBS at a concentration of 0.5 mg/mL.*

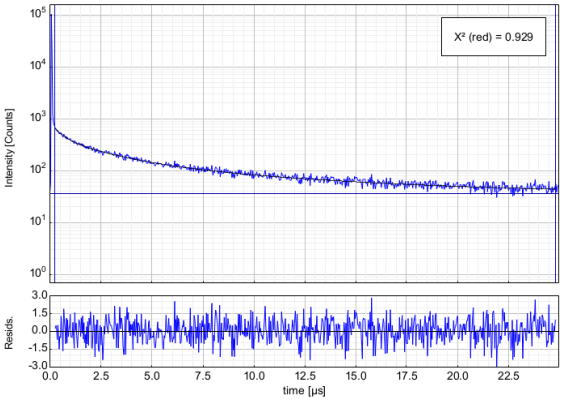

Parameter	Value	Conf. Lower	Conf. Upper
A_1 [Cnts]	136.23	-4.63	+4.63
τ_1 [µs]	8.616	-0.298	+0.298
A_2 [Cnts]	259.3	-13.4	+13.4
τ_2 [µs]	2.163	-0.118	+0.118
A_3 [Cnts]	209.1	-35.4	+35.4
τ_3 [µs]	0.4538	-0.0974	+0.0974
Bkgr. Dec [Cnts]	35.99	-1.32	+1.32

Figure S20. *Left: Time-resolved photoluminescence decay of* ***NP$_{core}$*** *including the residuals (λ_{exc} =376.7 nm, λ_{em}=500 nm). Right: Fitting parameters including pre-exponential factors and confidence limits.* ***NP$_{core}$*** *were suspended in aerated 10% PBS at a concentration of 0.5 mg/mL.*

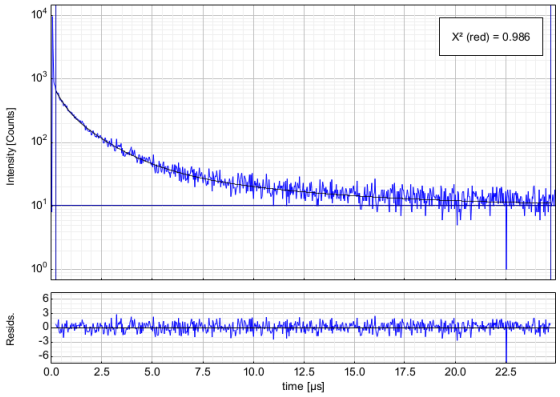

Parameter	Value	Conf. Lower	Conf. Upper
A_1 [Cnts]	43.09	-3.65	+3.65
τ_1 [µs]	6.469	-0.465	+0.465
A_2 [Cnts]	304.6	-14.0	+14.0
τ_2 [µs]	1.6042	-0.0654	+0.0654
A_3 [Cnts]	299.6	-36.3	+36.3
τ_3 [µs]	0.4273	-0.0602	+0.0602
Bkgr. Dec [Cnts]	10.169	-0.720	+0.720

Figure S21. *Left: Time-resolved photoluminescence decay of* ***NP$_{core}$*** *including the residuals (λ_{exc} =376.7 nm, λ_{em}=600 nm). Right: Fitting parameters including pre-exponential factors and confidence limits.* ***NP$_{core}$*** *were suspended in deaerated 10% PBS at a concentration of 0.5 mg/mL.*

7. Transmission Electron Microscopy (TEM) experiments with cells

HeLa cells were maintained in DMEM (Dulbecco's modified Eagle's Medium) containing 1% glutamine, with 1% non-essential amino acids, 1% penicillin-streptomycin, 1% sodium pyruvate, and 10% FBS (fetal bovine serum) in a humidified atmosphere (5% CO_2) at 37 °C. For the TEM experiments, HeLa cells were plated at 200,000 cells per dish in 35 mm round plastic dishes 18 h prior to treatment. At that point $\mathbf{NP_{shell}}$ were used for the incubations on the cells for 30 min. The cells were washed three times with DPBS and then fixed with 2% glutaraldehyde in 0.1 M sodium cacodylate buffer at pH = 7.4 (SC buffer) on ice for 2 h. After washing three times with 0.1 M SC buffer for 5 min, the cells were post-fixed with 1% osmium tetroxide in 0.1 M SC buffer for 1 h on ice. The cell pellets were washed three times with 0.1 M SC buffer for 5 min, followed by a quick rinse in distilled H_2O. Cell pellets were stained with 2% uranyl acetate (UA) for 1 h on ice, then dehydrated in a graded series of ethanol (50%, 70%, 90% and two times 100%) for 5-8 min, and dried in acetone at room temperature. The cell pellets were infiltrated by a 50:50 dry acetone/Durcupan solution for 1-2 h on a shaker, followed by 100% Durcupan overnight and two further treatments of 100% Durcupan the next day. Finally, cell pellets were embedded in Durcupan and incubated at 60 °C for 36-48 h. Ultrathin sections (around 60 nm) were cut and examined by electron microscopy.

8. Two-Photon Laser Scanning Microscopy (TPLSM) experiments

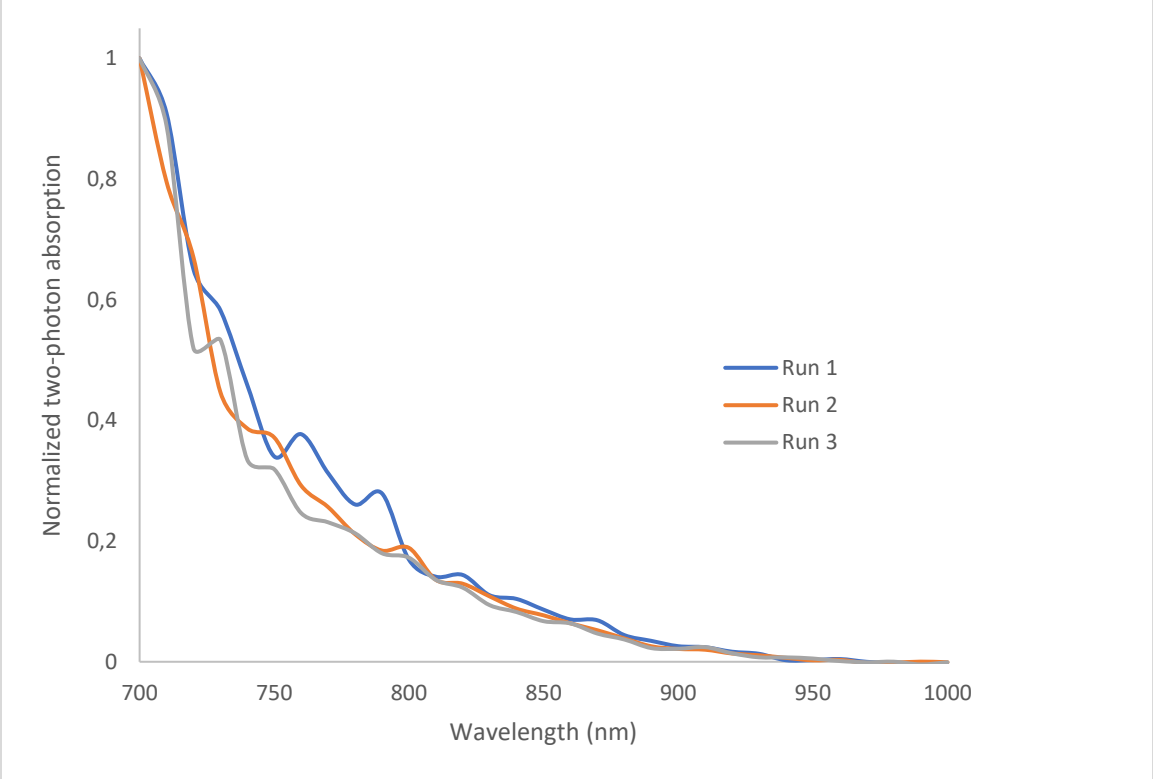

Figure S22. *Degenerate two-photon absorption spectrum of* $\mathbf{M_{Pt}}$ *in fluid* CH_2Cl_2 *at room temperature.*

Degenerate two-photon absorption spectroscopy protocol

The degenerate two-photon absorption spectrum of $\mathbf{M_{Pt}}$ was measured using a custom-built spectrometer. The light source was a Coherent Chameleon Ultra II laser, which generates 140-190 fs pulses with an 80 MHz repetition rate in the 680-1080 nm spectral range. The laser power after objective was measured for each wavelength and a table for the ratio of the powers measured in the setup and power after objective was generated. This was a necessary step since transmission of optical elements are slightly different for different wavelengths. Beam was expanded to overfill the microscope objective pupil aperture and was then directed into a microscope objective (Olympus, LN10XIR), which focused the beam into a rectangular Quartz cuvette (WPI, 2 mm path, 0.7 mL volume) filled with the sample solution. We then tuned the illumination beam through the desired tuning range in 10 nm steps. At each step we averaged 1000 samples from the PMT and 100 readings from the laser reference power meter, in addition we collected laser repetition rate, wavelength and spectral bandwidth. The emission was collected in epi-

fluorescence mode, reflected from two dichroic mirrors with cutoffs of 678 nm (Semrock, FF678-Di01-25x36) and 735nm (Semrock, FF735-Di01-25x36) and subsequently passed through a fluorescence bandpass filter, Semrock FF01-525/50-25. Finally, the fluorescence was detected using a photomultiplier (PMT; Hamamatsu, H11461-03). The photocurrent from the PMT and the laser power meter readings were acquired using a data acquisition board (National Instruments). The normalized two-photon absorption cross section is given by the following relation:

$$\frac{\sigma(\lambda)}{\sigma(\lambda_m)} = \frac{F\tau\lambda P^2}{F_m\tau_m\lambda_m P_m^2}$$

where F is the collected time averaged fluorescence, σ is the two-photon absorption cross section, τ is the pulse width, λ is the wavelength, P the is beam power and the subscript m indicates the related values for the maximum absorption cross section of the sample.

TPLSM experiments with HeLa cells

For TPLSM, HeLa cells were plated at 200,000 cells per dish in 35 mm round plastic dishes 18 h prior to treatment. At that point, **NP_{shell}** were used for incubation of the cells for 60-75 min. The cells were then placed in modified Tyrode's solution (in mM: NaCl 140, KCl 5, $MgSO_4$ 1.2, $CaCl_2$ 2.5, Glucose 5, HEPES 5, pH 7.4) at room temperature for imaging with a two-photon laser scanning microscope.